

Fabrication of Titania Tubules with High Surface Area and Well-Developed Mesostructural Walls by Surfactant-Mediated Templating Method

Tianyou Peng,^{*,†,‡} Akira Hasegawa,[‡] Jianrong Qiu,[§] and Kazuyuki Hirao^{†,‡,§}

Department of Materials Chemistry, Graduate School of Engineering, Kyoto University, Yoshida, Sakyo-ku, Kyoto 606-8501, Japan, Fukui Institute For Fundamental Chemistry, Kyoto University, 34-4 Takano-Nishihiraki-cho, Sakyo-ku, Kyoto 606-8103, Japan, and Photon Craft Project, ICORP, Japan Science and Technology Corporation (JST), Keihanna-Plaza, Super-Lab. 2-5, 1-7 Hikaridai, Seika-cho, Kyoto 619-0237, Japan

Received August 9, 2002. Revised Manuscript Received November 26, 2002

Titania microtubules with high specific surface areas and well-developed framework mesopores forming the tubular walls by a surfactant-mediated template in the sol–gel process were fabricated in a laurylamine hydrochloride (LAHC)/tetra-*n*-butyl-orthotitanate (TBOT) system. The outer diameter and the wall thickness of titania microtubules are 2–8 and 0.2–2 μm , respectively. The walls of the microtubules consisted of nanochannels with exceptionally uniform pore size. This technique is a convenient and facile procedure for fabricating hierarchical ordered hollow tubules. The possible mechanism of the formation of the microtubules in the present system was discussed in detail.

Introduction

Recently, considerable attention has been devoted to the fabrication of hollow tubules due to their novel properties and the potential applications in optics, electronics, photocatalysts, and separation science. Thus, enormous work has been directed to fabricating hollow tubules of metal oxides with diameters ranging from micrometers to nanometers.^{1–8} Generally, template-based approaches have been utilized to fabricate tubular materials, such as carbon nanotubes,^{1,2} alumina porous membranes,^{3,4} gelator fibers,^{5,6} and inorganic⁷ and organic crystals.⁸ In these cases, the hollow metal oxide tubules are formed on removal of the template. The Mobil research group has synthesized ordered tubules in condensed forms, that is, mesoporous materials (M41S family) by using surfactant assemblies as a template.^{9,10} Since then, a variety of mesoporous ma-

terials with condensed forms of unit cylindrical structure have been synthesized.^{11–15} On the basis of this strategy, a novel approach based on the self-assembly of surfactant in the liquid phase has also been applied to fabricate single or bundles of a few tubular structures;^{6–21} for example, a liquid-crystal membrane of trimethylammonium bromide was used as a template to synthesize single and bundles of several hollow tubules of aluminosilicate and pure silica by a hydrothermal method. The tubules with MCM41 structural walls have diameters of ca. 3 μm .¹⁶ The same group has also prepared silica tubule with diameter between 50 and 150 nm by a similar procedure.¹⁷ Multiwall V_2O_5 tubules with an inner diameter of 5–50 nm were also obtained by a post-hydrothermal treatment of the alkylamine-intercalated form as structure-directing agents.¹⁸ Yada et al. used urea as homogeneous precipitation agents to synthesize rare earth oxide nanotubule templating by dodecyl

* Corresponding author. E-mails: typeng@collon1.kuic.kyoto-u.ac.jp; typeng@ifc.or.jp.

[†] Department of Materials Chemistry, Graduate School of Engineering, Kyoto University.

[‡] Fukui Institute For Fundamental Chemistry, Kyoto University.

[§] Photon Craft Project, ICORP, Japan Science and Technology Corporation.

(1) Rao, C. N. R.; Satishkumar, B. C.; Govindaraj, A. *Chem. Commun.* **1997**, 1581.

(2) Satishkumar, B. C.; Govindaraj, A.; Nath, M.; Rao, C. N. R. *J. Chem. Mater.* **2000**, *10*, 2115.

(3) Lakshmi, B. B.; Dorhout, P. K.; Martin, C. R. *Chem. Mater.* **1997**, *9*, 857.

(4) Zhang, M.; Bando, Y.; Wada, K. *J. Mater. Sci. Lett.* **2001**, *20*, 167.

(5) Jung, J. H.; Shinkai, S.; Shimizu, T. *Nano Lett.* **2002**, *2*, 17.

(6) Kobayashi, S.; Hanbasa, K.; Nakasaki, N.; Kimura, M.; Shirai, H. *Chem. Mater.* **2000**, *12*, 1523.

(7) Hippe, C.; Wark, M.; Lork, E.; Schuz-Ekloff, G. *Microporous Mesoporous Mater.* **1999**, *31*, 235.

(8) Miyaji, F.; Tatsumatsu, Y.; Sayama, Y. *J. Ceram. Soc. Jpn.* **2001**, *19*, 924.

(9) Kresge, C. T.; Leonowicz, M. E.; Roth, W. J.; Vartuli, J. C.; Beck, J. S. *Nature* **1992**, *359*, 710.

(10) Beck, J. S.; Vartuli, J. C.; Roth, W. J.; Leonowicz, M. E.; Kresge, C. T.; Schmitt, K. D.; Chu, C. T. W.; Olson, D. H.; Sheppard, E. W.; McCullen, S. B.; Higgins, J. B.; Schlenker, J. L. *J. Am. Chem. Soc.* **1992**, *114*, 10834.

(11) Ramann, N. K.; Anderson, M. T.; Brinker, C. J. *Chem. Mater.* **1996**, *8*, 1682.

(12) Tanav, P. T.; Pinnavaia, T. J. *Science* **1996**, *271*, 1267.

(13) Huo, Q.; Feng, J.; Shuth, F.; Stucky, G. D. *Chem. Mater.* **1997**, *9*, 14.

(14) Attard, G. S.; Glyde, J. C.; Goltner, C. G. *Nature* **1995**, *378*, 366.

(15) Lu, Y.; Gabguli, R.; Drewien, C. A.; Anderson, M. T.; Brinker, C. J.; Gong, W.; Guo, Y.; Soyey, H.; Dunn, B.; Hoang, M. H.; Zink, J. I. *Nature* **1997**, *389*, 364.

(16) Lin, H. P.; Mou, C. Y. *Science* **1996**, *273*, 765.

(17) Lin, H. P.; Mou, C. Y.; Liu, S. B. *Adv. Mater.* **2000**, *12*, 103.

(18) Spabr, M. E.; Bitterli, P.; Nesper, R.; Muller, M.; Krumelch, F.; Nissen, H. U. *Angew. Chem., Int. Ed.* **1998**, *37*, 1263.

(19) Yada, M.; Mihara, M.; Mori, S.; Kuroki, M.; Kijima, T. *Adv. Mater.* **2002**, *14*, 309.

(20) Adachi, M.; Harada, M.; Harada, T. *Langmuir* **2000**, *16*, 2376.

(21) Adachi, M.; Murata, Y.; Harada, T.; Yoshikawa, S. *Chem. Lett.* **2000**, 942.

sulfate assemblies.¹⁹ Laurylamine hydrochloride assemblies were also used as the template yielded silica and titania tubules with diameters of 5 nm.^{20,21}

Titania tubules have attracted a great deal of attention due to its excellent performance in semiconductor, photocatalyst, photoelectronics, photovoltaic cell, and deodorizing properties.^{3,4,6–9,21–25} The formation of titania tubules with mesoporous walls leads to increased surface area compared to rods or particles and should prove to be extremely beneficial for those applications. It has been proven that the photocatalytic activity is dependent on the crystalline phase and the specific surface area of the fibrous titania during the degradation of phenol.²⁵ Therefore, it is necessary to develop a facile pathway for synthesizing tubular titania with well-organized porous structures. Here, we describe a sol–gel method for fabricating titania microtubules with mesoporous walls as well as a large specific surface area by the surfactant-mediated template in a laurylamine hydrochloride (LAHC)/tetra-*n*-butyl-orthotitanate (TBOT) system. The obtained titania microtubules have a hierarchical organization of tubules-within-tubules with tubular nanochannels forming the walls of microtubules. The reaction conditions affecting the morphology and structural properties of the titania tubules were also investigated in detail.

Experimental Section

Analytical-grade laurylamine hydrochloride (LAHC) (Tokyo Kasei Co., Japan) and tetra-*n*-butyl-orthotitanate (TBOT) (99.99%, Tokyo Kasei Co., Japan) were used in this study. Typically, TBOT was added dropwise into 0.10 M LAHC aqueous solution (adjusted to pH 4.0 with HCl aqueous solution) under vigorous stirring at room temperature. The mole ratio of TBOT to LAHC was adjusted to 4–12. Since the hydrolysis and polycondensation reaction of TBOT are rather fast in water, the addition of TBOT should be very slow. The mixture became a translucent emulsified solution in the early stages of the reaction. And then the mixture became a white turbid slurry upon addition of TBOT. After continuous stirring for another 4 h, the white slurry was placed quietly for 24 h at 313 K in a closed container to further hydrolyze and condense as well as obtain rigid tubules. And then the precipitate was filtered and washed with ethanol and dried in an oven at 313 K for 1 week. To obtain the final anatase phase microtubules with nanochannel porous walls, the as-prepared products were calcined at different temperatures for 5 h under an ambient atmosphere. Structure phase analysis with the X-ray diffraction (XRD) method was performed on a Rigaku Rint-1400 X-ray diffractometer with Cu K α radiation ($\lambda = 0.15418$ nm). A continuous scan mode was used to collect 2θ with a low angle of $0.5\text{--}8^\circ$ and wide angle of $10\text{--}70^\circ$ was carried out. Scanning electron microscopy (SEM) was carried out on an Hitachi S-510 scanning electron microscope. Transmission electron microscopy (TEM) studies were carried out on an Hitachi JEM-100CX electron microscope. Nitrogen adsorption data were obtained on a micromeritics ASAP-2000 nitrogen adsorption apparatus.

Results

Figure 1 shows the SEM images of the titania tubules calcined at 773 K with different mole ratios of TBOT/

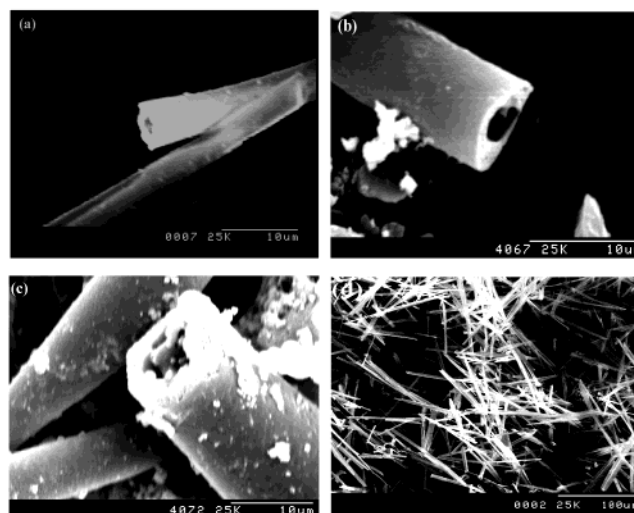


Figure 1. SEM images of titania microtubules calcined at 773 K, derived from [TBOT]/[LAHC] = 4 (a), 8 (b), and 12 (c) and the low magnification (d) of product derived from [TBOT]/[LAHC] = 4.

LAHC. As can be seen, the microtubules show its hollow nature with opened edges. It is evident that the samples derived from [TBOT]/[LAHC] = 4 exhibit a well-developed tubular morphology of 15–140 μm in length with the diameter and wall thickness between 2 and 8 μm and 0.2 and 2 μm , respectively. The outer surface of the tubules appear relatively smooth, and most of the tubules retained their tubular form without cracking even after heat treatment at 773 K for 5 h. The yields of microtubules can be observed from the low-magnification SEM image (Figure 1d). Upon increasing the mole ratios of TBOT/LAHC, the microtubules tend to form thicker walls and larger diameter of tubules, and the microtubules were contaminated with secondary aggregates of titania particles. Therefore, if otherwise mentioned, the sample described in the following section was derived from [TBOT]/[LAHC] = 4.

To inspect the processing conditions controlling the morphology and structure properties of the titania microtubules, the factors affecting the hydrolysis and condensation process were investigated in detail. It was found that the condition of preparation is important in the final formation of titania microtubules. Tubular products were obtained only under conduction of the reaction of hydrolysis and condensation of precursor (at pH 4.0) at room temperature as well as aging at 313 K. An elevated temperature is not beneficial for the formation of tubular products. In addition, no tubular materials can be obtained without LAHC. Therefore, the formation of titania microtubules is assumed to be closely related to the presence of LAHC as templating or mediating reagents in the sol–gel process.

Figure 2 shows the low-angle XRD pattern of the sample calcined at 773 K and the wide-angle XRD patterns (inset) of samples and those calcined at different temperatures. As can be seen, the as-prepared titania microtubules exhibit a broad diffraction XRD pattern (inset Figure 2a) characteristic of the single phase of anatase with low crystallinity. This fact is quite different from the previous results based on a sol–gel process by using titanium alkoxide as precursor in which the titania tubules have amorphous walls before

(22) Crauso, R. A.; Schattka, J. H.; Greiner, A. *Adv. Mater.* **2001**, 13, 1577.

(23) Imai, H.; Matsuda, M.; Shimizu, K.; Hirashima, H. *J. Chem. Mater.* **2000**, 10, 2005.

(24) Imai, H.; Shimizu, K.; Matsuda, M.; Hirashima, H.; Negashi, N. *J. Chem. Mater.* **1999**, 9, 2971.

(25) Deki, S.; Aoi, Y.; Kajinami, A. *J. Mater. Sci.* **1997**, 32, 4269.

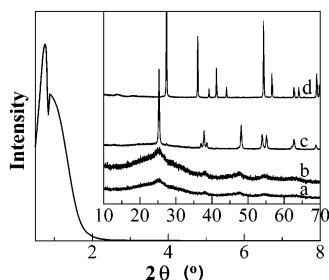


Figure 2. Low-angle XRD pattern of the calcined sample and wide-angle XRD patterns (inset) of samples as-prepared (a), calcined at 673 K(b), 773 K(c), and 1073 K(d); derived from [TBOT]/[LAHC] = 4.

calcination.⁸ But Adachi et al. have also obtained anatase titania nanotubules before calcination from the LAHC/titanium alkoxide system using titanium isopropoxide modified with acetylacetone (ACA) as the titanium source,²¹ which is very similar to our system. The possible reason is the existence of chloride because chloride ion has been proven to assist in the selective formation of crystalline rather than amorphous titania in the hydrolysis of titanium alkoxides.²⁶ More still remains to be learned about the direct formation mechanism of the crystalline structural walls of tubules in the present system. Even with calcination at 673 K, the product (Figure 2b) yet shows a similar diffraction pattern but with a relatively high crystallinity, and then it crystallized completely into the anatase structure after heat treatment at 773 K for 5 h. Upon increasing of the temperature to 1073 K, rutile phase became predominant. The other products derived from different ratios of [TBOT]/[LAHC] also show similar characteristics of XRD patterns. The mean crystalline size in the walls of titania microtubules were deduced according to the Scherrer equation using fwhm data of each phase. The calculated crystalline sizes (D_{khl}) of the samples as-prepared and calcined at 673, 773, and 1073 K are 2.6, 5.5, 9.7, and 35.9 nm, respectively.

The low-angle diffraction pattern (Figure 2) of the sample calcined at 773 K shows a broad diffraction peak corresponding to a d spacing of 12.2 nm with a broad shoulder. Such low-angle peaks at $2\theta < 5^\circ$ were not observed in titania nanotubules with a diameter of ca. 5 nm.²¹ Although analogous diffraction patterns have been observed for hexagonal mesostructures silica and its titanium-substituted derivative by using laurylamine-templating pathways,²⁷ we have not observed other high reflection peaks attributed to ordered mesoporous structures such as hexagonal, cubic, and/or lamellar structures. In addition, during TEM observation, the electron cannot transmit the walls and/or fragments of the microtubules, even when the transmission is operated at 200 kV, due to the large dimensions and thick walls; therefore, the microtubules have been treated with supersonic dispersion for 1 h to destroy the microtubule and thick wall structures, and then the product underwent TEM observation. The TEM image (Figure 1S) of fragments of microtubules after super-

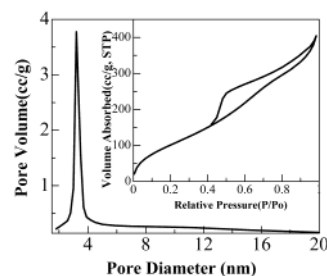


Figure 3. Pore size distribution and the liquid nitrogen adsorption-desorption isotherm (inset) of TiO₂ microtubules calcined at 773 K, derived from [TBOT]/[LAHC] = 4.

sonic treatment is given in the Supporting Information. As can be seen from Figure 1S, the nanochannels with ca. 3-nm diameter randomly disperse in the walls of microtubules. No other regular and/or periodical arrangements have been observed in the TEM images of fragments of microtubules. Thus, we think that the broadness of the single peak with a broad shoulder and absence of the other peaks in the low-angle range are related to the uniform pore size rather than the long-range ordered arrangement of pores in the walls of tubules.

Figure 3 shows the liquid nitrogen adsorption-desorption isotherm (inset) of the sample calcined at 773 K. It shows a type IV-like isotherm with a sharp inflection of nitrogen adsorbed volume at $P/P_0 = 0.42$ (type H2 hysteresis loop), indicating the presence of well-developed framework mesopores in the walls of microtubules. The hysteresis loop at high partial pressure ($P/P_0 > 0.8$) can be attributed to the capillary condensation of nitrogen in interparticle pores. The other samples derived from high mole ratios of [TBOT]/[LAHC] also show similar liquid N₂ adsorption character. In the hysteresis loop at high partial pressure, more contribution from interparticle pores can also be observed, which is consistent with the observations of SEM images (Figure 1b,c) in which microtubules coexist with a relatively large amount aggregates of particles. The BET surface area and pore volumes were calculated as large as 390 m²/g and 0.586 mL/g, respectively; the evaluation of the surface area of the sample calcined at 773 K allows us to compare it to the previously reported mesoporous titania materials. Although the concentration of surfactant in the present work is much lower than that in the previous work, the surface area is much higher than that of the mesoporous titania derived from the neutral laurylamine/ethanol/TBOT system (246 m²/g calcined at 573 K).²⁸

The pore size distribution (see Figure 3) of the sample calcined at 773 K was obtained by the BJH (Barret-Joyner-Halenda) method from the adsorption branch of the isotherm. The pore size distribution for the calcined sample was very sharp with a BJH pore diameter at ca. 3.2 nm, which is reasonable because it is a little less than twice the lengths of organic chains of LAHC (3.34 nm),²⁰ indicating an exceptionally uniform nanochannel pore size. The pore diameter is also similar to the 3-nm value by the observation of TEM (Figure 1S). The fidelity of pore distribution (ca. 0.45 nm at half-maximum) is similar to that observed in

(26) Henry, M.; Jolivet, J. P.; Livage, J. In *Role of Complexation in the Sol-Gel Chemistry of Metal Oxides, Ultrastructure Processing of Advanced Materials*; Uhlmann, D. R., Ulrich, D. R., Eds.; John Wiley & Sons: New York, 1992; Chapter 3.

(27) Tanev, P.; Chibwe, M.; Pinnavaia, T. J. *Nature* **1994**, 368, 321.

(28) Wang, Y. D.; Ma, C. L.; Sun, X. D.; Li, H. D. *Mater. Lett.* **2002**, 54, 359.

mesoporous silica prepared by electrostatic templating from alkylammonium ions,⁹ and better than that by electronically neutral templating from a primary amine.²⁷ The cylindrical- to hexagonal-shaped channels with uniform pore diameters but lack of long-range packing order have also been observed for hexagonal-like M41S silicates in which silicate anions bind electrostatically to separated rodlike micelles of quaternary ammonium ions that subsequently aggregate into mesostructure.²⁹ Furthermore, the ratio (1.50 nm) of total pore volume (0.586 mL/g) and BET surface area (390 m²/g) was found to be close to the value of $r_{av}/2$ (r_{av} is the BJH average pore radius (2.91 nm)), implying the pores in the walls of microtubules possess tubular or cylindrical channels.³⁰ Considering the large difference between d spacing (12.2 nm) and the pore diameter (3.2 nm), we conclude the following: (1) the afforded microtubules walls have very thick walls between the cylindrical nanochannels; (2) the pore channels are exceptionally uniform in diameter, although there is a lack of long-range packing order; (3) the arrangement of cylindrical nanochannels in microtubular walls is random (refer to Figure 1S); and (4) the broad lines observed in low-angle XRD patterns arise from the random arrangement of the cylindrical nanochannels in the walls of titania microtubules.

Discussion

A simple theory of micellar structure has been developed based on the geometry of micellar shape and the shape of the surfactant molecule. The packing parameters (P value) are defined as V_H/a_0l_c in which V_H and l_c are the molecular volume and the extended length of the hydrophobic chain of the structure, respectively. a_0 represents the area occupied by a surfactant molecule on the surface of the molecular assemblies. For spheres, $P < 0.33$; for cylinders, $0.33 < P < 0.5$; for bilayers, $P > 0.5$. According to $l_c = 1.67$ nm, $V_H = 0.350$ nm³, and $a_0 = 0.33$ nm²,^{2,20} the P value for LAHC is calculated as 0.64, indicating the formation of lamellar phase. When the concentration of LAHC is reduced to 0.1 M (pH 4–5), globular aggregates rather than liquid-crystal phase were formed, which are presumed to be finely divided bilayerlike assemblies in a spongelike phase according to Adachi et al.²⁰ Generally, these bilayer-like or sponge-like assemblies formed at this low concentration of surfactant have no cylindrical micelle or liquid-crystal phase, which is necessary for the formation of nanochannels in walls as well as microtubules described as above, but there are also many publications reported about MCM-41 silica synthesis from a low initial concentration of surfactant.^{9,10} It is well-known that there is no liquid-crystal phase in solution prior to addition of silica in these cases, but yet MCM-41-like liquid-crystal products form. This implies that the interfacial interactions between surfactant and silica become increasingly important, the silica and surfactant cooperatively organizing into an inorganic surfactant liquid-crystal phase during the progress of the reaction. Furthermore, when electrolytes are added to trimethylammonium bromide solution, a spherical-to-cylindrical micellar

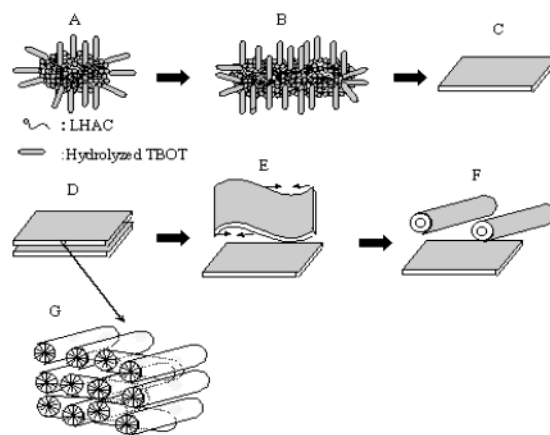


Figure 4. Proposed formation processes of the microtubules. (A) Globular aggregates containing LAHC and hydrolyzed TBOT. (B) Aggregates enlarged in size. (C), (D) Mixed lamellar liquid-crystal phase membrane containing rodlike micelles. (E) Charge imbalance resulting in membrane curvature. (F) Further bending into tubules. (G) Random and segregated arrangement of rod micelle layers which are separated by bilayers of LAHC from bulk solution.

transition has also been observed. A liquid-crystal phase transformation mechanism involving an anisotropic trimethylammonium bromide membrane-to-tubule phase change is proposed for the formation of hollow silica and aluminosilicate microtubules with the walls of the tubule consisting of MCM-41 coaxial cylindrical pores.¹⁶ We propose that an analogous mechanism may take place in the present system due to our sample possessing a similar microstructure.³¹ The proposed formation mechanism is summarized as shown in Figure 4.

Under acidic conditions, titanium alkoxide is first hydrolyzed in the early stages of adding TBOT. The partially hydrolyzed TBOT (defined as I^+) will be positively charged.³ Those charged species I^+ combined with the surface of the bilayer-like assemblies and formation of aggregates through chloride ion (Cl^-) mediate the interaction between the laurylamine surfactant and charged hydrolytic species (I^+) ($RNH_3^+Cl^-I^+$) by weak H-bonding forces (Figure 4A).³² The geometric matching between the LAHC and the hydrolyzed titanium alkoxide species enable the planar surface of LAHC aggregates to be covered. The surface of bilayer assemblies of LAHC is stabilized by the progress of the condensation reaction of titanium species, but the edge portions of the bilayer assemblies have no such matching. Thus, the edge portions are relatively unstable; this leads to the interlayers combining along the edges of the assembly and enlargement of the layers (Figure 4B). And then the condensation reaction proceeds to interlayer polymerization and subsequently the bilayer-like aggregates rearrange into lamellar-like liquid-crystal

(29) Davis, M. E.; Chen, C. Y.; Burkett, S. L.; Lobo, R. F. *Mater. Res. Soc. Symp. Proc.* **1994**, 346, 831.

(30) Lippens, B. C.; De Boer, J. H. *J. Catal.* **1965**, 4, 319.

(31) Although we did not observe any separate intermediate products, and also did not apply instrumental methods such as small-angle XRD, to capture the intermediate phase in our system, enormous research results concerning the fabrication of MCM-41 mesoporous materials and nanotubules templating by self-assembly of surfactant can provide a reasonable explanation of the formation of the special structure obtained by us. Especially, the conditions of reaction and the results in the present work are very similar to those in refs 20, 21, and 16. On the basis of these facts, we deduced the formation mechanism. Certainly, the precise mechanism should be further investigated.

(32) Schacht, S.; Huo, Q.; Voigt-martin, I. G.; Stucky, G. D.; Schuth, F. *Science* **1996**, 273, 768.

phases (Figure 4C). In the meantime, upon the hydrolyzed titanium alkoxide species further penetrating the lamellar-like liquid-crystal phases, those aggregates have large a_0 , and the P value is decreased and locates on the borderline between lamellar and rod micellar phase. Upon further interlayer combination and cross-linking between adjacent hydrolyzed titanium alkoxide species, the P value will further decrease and locate in the rod micellar phase region. This would proceed cooperatively with partial release of the surfactant molecules and then in the lamellar assemblies some aggregates converted into rodlike micelles. Finally, a mixed lamellar liquid-crystal phase membrane formed in which layers of rodlike micelles are separated by bilayers of surfactant and water (Figure 4D). The layered structure can be stabilized by electrostatic repulsion force between the membrane layers.

Because the membrane layers are intrinsically anisotropic, upon dropwise addition of TBOT, more and more charged hydrolyzed titanium alkoxide species combine with and/or penetrate the liquid-crystal membrane, and charge imbalance will emerge on the membrane surface, which should favor the curvature of the membrane along only one direction (the transrod direction) (Figure 4E) and then bend fully the membrane into tubules (Figure 4F). The driving forces arise from the charge imbalance at the lamellar membrane surface, which is associated with the rates of condensation and hydrolysis of precursor as well as the combination of positively charged species with liquid-crystal membrane.

Let us consider the formation and arrangement of rodlike micelles in the liquid-crystal membrane. The low surfactant concentration results in our inability to obtain microtubules with periodical MCM-41 walls. As the reaction progresses, further condensation of the hydrolyzed titanium species occurs in the interstitial spaces of the randomly arranged flexible micelles in the liquid-crystal membrane, and if the rate of condensation is suitable, those random rodlike micelles in the membrane may be packed into a more regular arrangement. The condensation of inter-rod titanium species is thought to be a primary driving force for this packing trend. Unfortunately, the relatively fast condensation in the present system leads to the rodlike micelles not having enough time to arrange in an orderly fashion. Therefore, we think the rodlike micelles are in a random arrangement in the liquid-crystal membranes (Figure 4G). It should be noticed that this kind of arrangement does not affect the pore size, which is determined by the diameter of the templating micelles. Thus, upon removal of surfactant template by subsequent thermal treatment, the hollow inorganic microtubules can be obtained, and the framework-confined mesopores in the walls of microtubules maintain an exceptionally uniform nanochannel pore size but lack long-range order; the results of N_2 adsorption (Figure 3) and TEM observations (Figure 1S) of the fragments of microtubules after supersonic treatment have already proven this deduction. Furthermore, the nanochannels along the walls of microtubules contribute to the total surface area. This is the reason the TiO_2 microtubules have a relatively high surface area as indicated above.

Two direction factors are crucial to the formation of microtubules. One is the geometric matching between

the surfactant molecules and the titanium-hydrolyzed species as well as the static packing condition of the hydrophobic tail of the surfactant molecule to the aggregate shape, which concerns the formation of a large-sized liquid-crystal membrane. The other is the rate of condensation and hydrolysis of precursors as well as the rate of aggregation of positively charged species to liquid-crystal membranes, which will maintain the formed special liquid-crystal membranes and bend them into microtubules. Therefore, we think that a suitable condensation is necessary, so as to leave enough time for the soft membrane to bend into tubules, before the substantial polymerization of hydrolyzed titanium species result in a rigid-unbending structure. For the same reason, an elevated temperature is not beneficial for the formation of microtubules as indicated above; the condensation reaction under the elevated temperature is too fast, so the species derived from the hydrolysis of titanium alkoxide could not be directed into a tubular structural arrangement by the surfactant molecules. In fact, the original intention of the present work is to fabricate TiO_2 nanotubules according to ref 20 by just the TEOS being replaced with TBOT. Accidentally, the present findings were observed by slightly changing the reaction conditions in ref 20 (such as the reaction temperature being set at room temperature following aging at 313 K for 1 day and the original pH of LAHC being adjusted to 4.0 by HCl). Due to the relatively large spatial molecular structure of TBOT, the combination and geometric matching between the hydrolyzed titanium alkoxide species and LAHC are inferior to those of TEOS during the formation stages of $RNH_3^+Cl^-I^-$; the packing parameter values in this stage do not decrease as much compared to the values in the rod region, as described in ref 20. Furthermore, the fringe portions of the bilayers assembly are more unstable due to the lack of geometric matching; in addition, TBOT possesses a much more rapid rate of hydrolysis and condensation than TEOS. Those factors are beneficial for the formation of more and more interlayer combinations along edges of the assembly and enlarge the layers in size and then the bilayerlike aggregates rearrange into larger lamellar-like liquid-crystal phases (as shown in Figure 4B,C) rather than the bilayerlike aggregates converting to a single rod shape as mentioned in ref 20. On the other hand, the slightly higher acid in the LAHC solution is also beneficial for the formation of $RNH_3^+Cl^-I^-$ (Figure 4A) and the charge imbalance emerging in the membrane surface, which should favor the curvature of the membrane and then bend fully the membrane into tubules (as shown in Figure 4E,F). Finally, the TiO_2 microtubules rather than nanotubules can be fabricated. In our opinion, a slow adding strategy, room-temperature hydrolysis, and condensation as well as long-term aging is necessary for the formation of microtubules. Furthermore, single nanotubules of titania can also be formed if the condensation rate is suitable compared with the hydrolysis rate and the geometric matching between the alkoxide and LAHC is suitable. In fact, Adachi et al. has already synthesized nanotubules by slowing down the rate of hydrolysis and condensation using titanium isopropoxide (TIPO) modified with ACA as a titanium source in a very similar system.²¹ The reason for the formation of nanotubules

rather than microtubules in that system may be consist of the following: compared with the present system, the modification by ACA markedly slows down the rates of hydrolysis and condensation of TIPO, which delay the enlarging of the lamellar-like liquid-crystal phases during the stages represented in Figure 4B–D; this complexation is similar to the situation of TEOS to some extent. In addition, although the species of TIPO modified by ACA has a large spatial hindrance compared to TBOT (which affect the geometric matching), it also markedly enlarges the a_0 value during the combination and the geometric matching stages. Although the P value is located in the lamellar region before the addition of TIPO modified with ACA as mentioned above, it decreases similarly to the values in the rod region upon combination and geometric matching between the hydrolytic species of TIPO modified with ACA and LAHC. Those factors mentioned above favor the formation of segregated rodlike micelles instead of a large liquid-crystal membrane like the TBOT situation mentioned in the present system. And then, the surface of the rod is covered by hydrolytic species of TIPO modified with ACA and is stabilized by the progress of the polycondensation of titanium alkoxide. Those struc-

tures remained constant through the drying and calcination processes, and finally TiO_2 nanotubules can be fabricated.

Conclusion

Titania microtubules with high surface area and well-developed cylindrical nanochannels in the walls were fabricated by using LAHC as the template in the LAHC/TBOT system. Those hierarchical organized structures of microtubules with cylindrical nanochannels walls should prove to be extremely beneficial for catalysts, photoelectronics, and separation applications. Although the formation mechanism of these fascinating structures is still not completely understood, we believe that this novel procedure provides a simple route to fabricating other special hierarchical order mesoporous materials for various applications.

Supporting Information Available: TEM image of fragments of microtubules after supersonic treatment for 1 h (PDF). This material is available free of charge via the Internet at <http://pubs.acs.org>.

CM020828F